A novel method to predict the thermal conductivity of nanoporous materials from atomistic simulations

Julien Morthomas, William Gonçalves, Michel Perez, Geneviève Foray, Christophe Martin, Patrice Chantrenne

Version of Record: https://www.sciencedirect.com/science/article/pii/S0022309319302364
Manuscript_755cbcb80f6c7a1d73bf3fe7340579c7

A novel method to predict the thermal conductivity of nanoporous materials from atomistic simulations

Julien Morthomas[1*], William Gonçalves[1,2], Michel Perez[1], Geneviève Foray[1], Christophe L. Martin[2] and Patrice Chantrenne[1]
[1] *INSA de Lyon, Université de Lyon, MATEIS, UMR CNRS 5510, 69621 Villeurbanne, France*
[2] *Université Grenoble Alpes, CNRS, SIMaP, F-38000 Grenoble, France*

ABSTRACT:

The low density (smaller than 10% of the bulk density) and the nanostructured porosity of silica aerogels provide their extremely low thermal conductivities but also impact their poor mechanical properties. Atomic scale simulation is the appropriate tool to predict the thermal and mechanical properties of such materials. For such simulations, the interatomic potential should be carefully chosen to ensure result validity but also reasonable computational times. A truncated BKS potential has been used for aerogels as it fairly reproduces the nanostructure. It allows reducing the computational time by a 3000 gain factor on the CPU time per atom per step compared to the original BKS interatomic potential while predicting correctly the mechanical properties. However, when it comes to skeletal thermal conductivity of nanoporous silica, the associated computation times are too large for a representative volume. This is due to the low thermal diffusivity of the material. Here, a new method that takes advantage of the amorphous structure of silica and the diffusive nature of phonon heat transfer at the scale of an aerogel aggregate is proposed. The time dependent temperature profile in the system obtained from Non-Equilibrium Molecular Dynamics simulations is compared to the classical solution of the thermal diffusion equation and an identification procedure is used to determine the thermal conductivity of silica aerogels.

Keywords: silica aerogels, thermal conductivity, nanoscale, molecular dynamics.

1. Introduction

Silica aerogels are highly porous materials (more than 90% porosity) with pore size distribution of the order of a few nanometers. Such a size gives silica aerogels extremely low values of thermal conductivity, which is interesting if they are used as high-performance thermal insulators. However, these properties are obtained at the expense of their mechanical properties. Due to their nanostructure, the understanding and the prediction of their properties require atomic scale simulations. As silica aerogels are a porous heterogeneous material, the representative volume of the matter that has to be considered to predict its properties should contain several millions of atoms. With such a number of atoms, molecular dynamics simulations remain appropriate. However, the choice of an interatomic potential is challenging since the computational time has to be minimized.

Silica is a polar material, each atom thus carries an equivalent charge, inducing long range Coulombic interactions. Those have to be accounted for to calculate interatomic forces. Electrostatic forces have long-range interactions, which are costly in term of computation time. Using a BKS potential [1], Rajappa *et al.* [2] have shown that the contribution of long-range Coulomb interactions to the total energy is lower for the amorphous phase than for the crystalline phase at the same density. This result is coherent with the previous work done of Carré *et al.* [3] who proposed a BKS potential with truncated coulomb interactions to successfully predict the static and dynamic properties of bulk silica. Recently, Gonçalves *et al.* [4] investigated the properties of $(SiO_2)_n$ clusters and silica aggregates. For small aggregates of silica, the truncated BKS potential leads to the same[1] structural properties and surface energies as compared to the original BKS potential. This means that significant reduction of computation time (evaluated to a gain factor of 3000 on the CPU time per atom per time-step) is possible even when the ratio between the surface to the volume ratio of material increases drastically as for silica aerogels. Gonçalves *et al.* [5,6] further used the truncated BKS potential to generate realistic silica aerogel structures. They have shown that the representative volume that has to be used to predict reliable mechanical properties of such material is of the order of 80^3 nm^3. This is much larger than the maximum volume (20^3 nm^3) previously reached to predict mechanical behavior of silica aerogel from molecular dynamics simulations [7–9].

Heat transfer in silica aerogel is a combination of radiative and conductive heat transfer, both of which are coupled. Coquart *et al.* [10] and Wei *et al.* [11] predicted the equivalent thermal conductivity of aerogels, solving the coupled radiative transfer and conduction heat transfer equations. Coquart *et al.* [10] assumed that aerogels are made of a net of connected silica spheres, which diameter varies between 5 and 10 nm and they accounted for a variation of the thermal conductivity with the sphere diameter. This is not coherent with experimental observation [12] showing that silica

* Corresponding author at : Université de Lyon, INSA-Lyon, CNRS, MATEIS, 25, Avenue Jean Capelle, 69621 Villeurbanne cedex, France.
E-mail address: Julien.morthomas@insa-lyon.fr (J. Morthomas).

aerogels may be considered as $(SiO_2)_n$ clusters connected via nanometric SiO_2 ligaments. Several authors have already used molecular dynamics simulations to predict the thermal conductivity of silica aerogel [9,13–16]. In these studies, due to computation time, the volume of the systems was smaller than 20^3 nm^3 and the minimum density is higher than the typical density of silica aerogels (around $70 - 250 kg.m^{-3}$). Thus these system are not large enough to accurately describe the typical pore size distribution (centered on 10nm) observed experimentally [12,17,18]. Truncated BKS potential proposed by Carré *et al.* [3] could open new avenue to calculate silica aerogel thermal conductivity at a reasonable cost. Although if this interatomic potential leads to appropriate surface properties [4], nanoporous silica aerogel structures and pore size distribution [5,6], it does not warrant that the value of the thermal conductivity is reliable. In addition, in order to calculate the thermal conductivity of the silica aerogels the same conclusion could be made as for the mechanical properties, where it is necessary to study a sufficiently representative volume close to 100^3 ^{3}.

Two methods based on molecular dynamics simulations are widely used to determine the thermal conductivity from molecular dynamics simulations [19]: Equilibrium Molecular Dynamics (EMD) and Non-Equilibrium Molecular Dynamics (NEMD). In EMD simulations, the instantaneous variation of the heat flux in a system at equilibrium is calculated; the thermal conductivity is then extracted thanks to the Green Kubo Formulae [20–23]. NEMD simulations are equivalent to well-known guarded hot plate experiments. It consists in simulating heat transfer in one direction of space by imposing a temperature difference between a hot zone and a cold zone. The technique to maintain the constant temperature in the hot and cold zones depends on the simulation strategy. Either the heat flux between the hot and cold zone is imposed [24–26], or the hot and cold zones are thermostated [27–30]. It has been shown by several authors that the two methods give consistent results [31–34]. EMD exhibits larger uncertainties than NEMD since it requires a larger number of time steps to calculate an accurate correlation function of the instantaneous heat flux. Moreover, it appears that when the system is not homogeneous, then significant differences may appear [35]. This is because the EMD method is based on the Green Kubo formula, which is only valid for homogeneous systems. In this study the NEMD method, detailed in section II.C.1., is used to determine the thermal conductivity of silica aerogels.

The duration of NEMD simulations (number of time steps) and thus the computation time is governed by the characteristic time, τ, to reach the steady state for heat transfer. To evaluate τ, we consider a solid system made of a continuous material. The system is defined by its volume, , which a characteristic length, , a specific heat, , a density, ρ and its thermal conductivity, λ. If the material is opaque (no radiative heat transfer) and if is much larger than the phonon mean free path of the material Λ, then the Fourier's law applies to describe heat transfer within this system. If the system, initially at a temperature , is placed in a heat source at temperature then the temperature of the system will tend towards the temperature of the medium. The duration of the transient state is proportional to the characteristic time

$$= \quad ^2/ \ .$$

For the silica aerogel systems studied here, the density varies between 2255 . $^{-3}$ (dense silica) and 250 . $^{-3}$ (silica aerogel which porosity is about 90%), and the characteristic length between 20 and 90 . At ambient temperature, the specific heat is equal to 720 . $^{-1}$. $^{-1}$. However, Molecular Dynamics (MD) simulations are based on the Newton equation and there is no quantification of energy, so whatever the temperature level, the specific heat of each atom is 3 (with k_b the Boltzmann constant), which is equivalent to a specific heat of 1240 . $^{-1}$. $^{-1}$. The thermal conductivity is approximately 1.5 $^{-1}$. $^{-1}$ for dense silica and we expect that it decreases for silica aerogels down to values of the order of 0.05 . $^{-1}$. $^{-1}$ [13–16]. Using these orders of magnitude, we may expect simulation durations should be performed within 10 to $100ns$. This would lead to prohibitive computation times that would prevent a large number of systems of being tested especially those close to 100^3 ^{3} in size.

A new simulation strategy to optimize the computational time and extract the value of the thermal conductivity from NEMD simulations with large volumes of nanoporous silica has been developed and is described in section II. This method is used to study the minimum size of the volume of silica aerogel that has to be considered to predict the thermal conductivity of silica aerogel which density is 250 . $^{-3}$. It is also used to assess the relationship between the silica aerogel density and its thermal conductivity. Results are compared to previous theoretical predictions and experimental values in section III.

2. Models and methods

2.1 Simulation strategy

Considering that silica aerogel has an amorphous structure, the phonon mean free path is of the same order of magnitude as the atomic distances and heat transfer through silica is diffused. Thus, during the transient state, the temperature profile in the system obtained with NEMD simulations should be the same than in an equivalent system made of a continuous material of the same geometry and thermal properties than the system described at the atomic system. To optimize the computational time, a three steps simulation strategy to calculate the thermal conductivity of silica aerogels has been developed here: (i) The evolution of temperature

profiles during the transient state is calculated by NEMD from silica aerogel simulation boxes. (ii) The evolution of the temperature profile is also calculated by solving the one dimension second order heat transfer differential equation (HTDE) based on a guess of thermal conductivity. (iii) The evolutions of these two temperature profiles are then compared in order to extract a new value for thermal conductivity λ by identification using a least mean square algorithm. Steps (ii) and (iii) are thus repeated until a satisfactory convergence for thermal conductivity is achieved. Details on these different steps are given below.

(i) We start from cubic simulation boxes of nanoporous silica of volume ^{3} with a prescribed density and equilibrated at 300 . A given energy quantity is removed from the cold zone and given to the hot zone at each time step using a velocity rescaled technic, see Fig. 1a. As periodic conditions are used, to avoid direct heat transfer from the hot to the cold zones, atoms have been fixed between these two zones. Thus, heat transfer may only occur between the two zones through the silica aerogel. The temperature profiles (,) are stored in regularly spaced slices at positions (the middle of each slice) of $4Å$ thickness and at different times . The value of the energy quantity and the number of time steps has to be adapted for each system size and density to ensure both a large enough temperature gradient compared to temperature fluctuations and a good convergence.

(ii) The temperature profiles (,) of a 1D system of length initially at temperature $(x,0) = 300$ (see Fig. 1b) is calculated at the same locations and times than for the NEMD simulation, solving the second order heat transfer differential equation (HTDE):

$$\rho c \frac{\partial T_s(x,t)}{\partial t} = \lambda \frac{\partial^2 T_s(x,t)}{\partial x^2}$$

To reproduce the same condition of heat transfer than for the MD simulations, the heat flux $= E/(L^2 \Delta t)$, with Δ the time step used in MD simulation, is imposed on both sides of the system:

$$x = \{0, L\}, \forall t: \ \lambda \frac{\partial T_s(x,t)}{\partial t} = \varphi$$

At the first time this step, a guess of the thermal conductivity λ is used ranging between 1.5 $^{-1}$ $^{-1}$ and 0.05 $^{-1}$ $^{-1}$.

(iii) Using a least mean square algorithm, a new value of the thermal conductivity is calculated by minimizing the functional

$$F(\lambda) = \sum_{i=1}^{n_a} \sum_{j=1}^{n_t} \left(T_s(x_i, t_j) - T_a(x_i, t_j) \right)^2$$

We observed that the temperature field calculated with MD simulations is submitted to fluctuations, $\sigma( ) \sim \sqrt{\ /\ }$ with the number of atoms and the temperature level. This is due to the fact that the number of atoms is relatively small. These fluctuations inhibit the functional to converge towards zero. The variation of the thermal conductivity between two iterations should decrease towards zero if there were no temperature fluctuations. Due to temperature fluctuations, when the iteration number is large enough, the thermal conductivity oscillates around a mean value with a relative variation of less than 1% which is the chosen convergence criterion. The quality of the results may be checked by looking at the mean deviation D between the temperature calculated using the HTDE and the one obtained from MD simulation. The mean deviation is divided by the mean value of the temperature fluctuation $\sigma(T_a)$ for the interpretation:

$$D = \frac{1}{\sigma(T_a) n_i n_j} \sum_{i=1}^{n_a} \sum_{j=1}^{n_t} \left| T_s(x_i, t_j) - T_a(x_i, t_j) \right|$$

where and are the number of slices and the number of consecutive time steps used for the summation average at the time , respectively. After convergence, should be almost equal unity. Values of much smaller than unity means that the numerical solution of the HTDE gives almost the same results than MD simulations despite the temperature fluctuations, which is not physical. This might happen if the number of times used for the comparison is too small. Values of much larger than unity means that the numerical solution of HTDE differs significantly from MD simulations. In that case, the two models might differ physically.

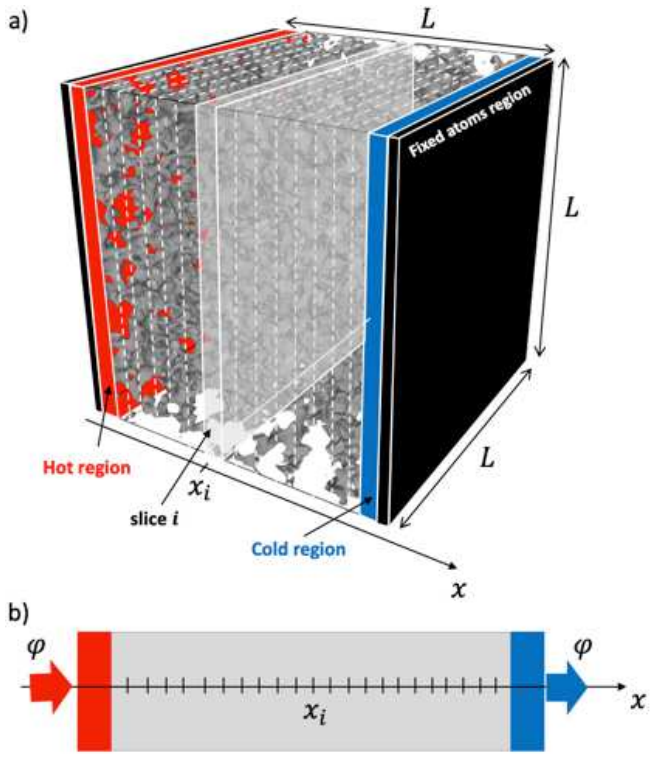

Fig.1. Configuration for a) the NEMD simulations and for b) the classical 1D transient simulation of heat transfer in a homogeneous continuous medium.

In step (i) and (ii), the initial temperature is chosen equal to 300 . However, as already stated, MD only solves the classical equation of Newton and no quantification of energy is accounted for. So, the comparison of MD results for the thermal conductivity is theoretically reliable (if the interatomic potential is accurate) for temperatures higher than the Debye temperature. In our case, our aim is to compare thermal conductivity values for different system sizes and densities. Qualitatively, the choice of the temperature range is not important. Choosing a higher temperature range would have resulted in higher temperature fluctuations. The ambient temperature offers a good compromise between the temperature gradient and temperature fluctuations.

2.2. Interatomic potential and boxes preparation

In this study, all MD simulations are performed using the Wolf BKS potential (van Beest, Kramer and van Santen), proposed by Carré *et al.* [3,36], which mainly differs from the original BKS potential by the introduction of a cut-off on Coulombic long-range interactions (shifted Wolf method [37]) and ensuring the continuity of both the potential and the force at the cut-off radius as proposed by Fennell et al. [38]. Fennell et al. [38] have shown very good agreement between this method and the full Ewald summation used for the original BKS potential. In a previous study [4], we confirmed the transferability of the potential of Carré *et al.* [3] for reproducing silica surface properties. The gain in computation time obtained by the truncation of Coulombic interactions opens the possibility to generate sufficiently large volumes of silica aerogel to account for the pore size distribution observed experimentally [5,6]. Further, Carré *et al.* [3] showed that the vibrational density of state is well reproduced in comparison with the original BKS. Moreover, considering the large surface to volume ratio of highly porous materials such as silica aerogels, it is critical that the interatomic potential be able to reproduce the structure and energy of amorphous silica surfaces. Both truncated and original BKS potentials have been extensively used to study the surface properties of amorphous silica [4,39,40]. Those studies suggest that the BKS potential is a reliable choice to investigate thermal properties of highly porous materials.

The Wolf BKS potential, proposed by Carré *et al.* [3], writes:

$$\Phi_{\alpha\beta}^{W-BKS}(r) = q_\alpha q_\beta e^2 W_w(r) G_w(r) + \left[A_{\alpha\beta} e^{-\frac{r}{\rho_{\alpha\beta}}} - \frac{C_{\alpha\beta}}{r^6} - \left(A_{\alpha\beta} e^{-\frac{r_{c,sh}}{\rho_{\alpha\beta}}} - \frac{C_{\alpha\beta}}{r_{c,sh}^6}\right)\right] G_{sh}(r)$$

where

$$W_w(r) = \left(\frac{1}{r} - \frac{1}{r_{c,w}}\right) + \frac{r - r_{c,w}}{r_{c,w}^2},$$

$$G_w(r) = e^{-\frac{\gamma_w^2}{(r-r_{c,w})^2}}$$

$$G_{sh}(r) = e^{-\frac{\gamma_{sh}^2}{(r-r_{c,sh})^2}}$$

α, β stand for Silicon or Oxygen and e is the elementary charge. Effective charge values, q_α, q_β, and parameters, $A_{\alpha\beta}$, $\rho_{\alpha\beta}$ and $C_{\alpha\beta}$ can be found in [1]. The expression $W_w(r)$ introduces a finite distance cut-off $r_{c,w}$ on the coulombic interactions and it ensures the continuity of both the potential and the forces at $r = r_{c,w}$ [37,38]. $G_w(r)$ and $G_{sh}(r)$ functions are introduced to smooth interactions at the cut-off distance $r_{c,sh}$ and $r_{c,w}$. Here, $r_{c,w} = 10.17\dot{A}$ and $r_{c,sh} = 5.5\dot{A}$ and the widths of the smoothing function are $\gamma_w = \gamma_{sh} = 0.5\dot{A}$ [36]. The original BKS potential, which pertains to the Coulomb-Buckingham type, does not tend to positive infinity as r tends to zero. Thus, atoms may approach too close from each other if the temperature or the pressure of the system are too high. This may induce chaotic dynamics. A solution proposed by Shcheblanov et al. [36], and adopted here, is to add a strong repulsive term for short range interactions:

$$\Phi_{\alpha\beta}^{rep}(r) = \left(\frac{D_{\alpha\beta}}{r}\right)^{12} + E_{\alpha\beta} r + F_{\alpha\beta}$$

where $D_{\alpha\beta}$, $E_{\alpha\beta}$ and $F_{\alpha\beta}$ parameters are listed in [36].

Simulations are performed with the Large-scale Atomic/Molecular Massively Parallel Simulator (LAMMPS) [41]. The integration of the equations of motion is achieved using a velocity-Verlet algorithm and a 0.25 timestep needed for stability. Temperature and pressure are respectively maintained by a Langevin thermostat and a Berendsen barostat.

Dense amorphous silica samples are prepared from melting of β-cristobalite cubic structures of 52728 atoms at 5000 K. The resulting silica liquid is then quenched to 300 K at 4.7×10^{12} . $^{-1}$. Simulations boxes are equilibrated during 200 in the NPT ensemble at 300 K and zero stress. This box is then replicated in the three directions of space in order to get the required system size. It is then equilibrated during 1 in the NPT ensemble at 300 K and zero stress. This procedure is similar to the "melt-quench-duplicate" procedure described in [42–44] and used to create "big samples" of metallic glasses. Periodic boundary conditions are used in all directions. The final amorphous silica box has a density of 2255 ± 1 . $^{-3}$.

Silica aerogel simulations boxes are generated with Kieffer's method [45] by isostatically and instantaneously stretching by approximately 10% by steps a dense amorphous silica box in all directions.

Between each stretch, a relaxation stage in the NPT ensemble is applied during 50 ps to maintain a 300 K temperature and a zero pressure. The stretching/relaxation stages are repeated until the desired density is reached. More details can be found in Gonçalves *et al.* [5]. With this method and the truncated BKS interatomic potential, the pore size distribution is around $10nm$ for a $\rho = 250\ kg.m^{-3}$. This pore size is comparable to the experimental values [12,17,18] as for commercial silica aerogel obtained from sol-gel process [46] and leading to monolith like aerogel particles or composite made of aerogels.

3. Results

3.1. Amorphous dense silica

The thermal conductivity of dense amorphous silica is calculated by two methods: first by using classical NEMD simulations and second by relying on the simulation strategy described in section II.A. The aim is to validate our simulation strategy for a simple and well-known case of dense amorphous silica.

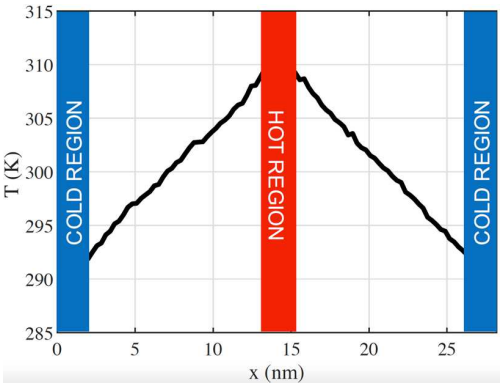

Fig.2. Temperature profile in steady state in a dense amorphous silica which section is 14.1×14.1 nm².

Formally, in the classical NEMD simulation, the average temperature gradient $\partial T/\partial z$ of the linear temperature profile is determined for the steady state conditions. The thermal conductivity is calculated from the Fourier's law:

$$\lambda = -\frac{\varphi}{\partial T/\partial z}$$

As the steady state has to be reached, the system size should not be too large to minimize the computation time. However, the value of the thermal conductivity is not reliable if the system size is too small. Thus, several simulations for different system sizes are run. The inverse of the thermal conductivity is plotted against the inverse of the system size to extrapolate the value of the thermal conductivity for an infinite system size. In our case, the optimum section of the system is 14.1×14.1 nm^2 and the system length varied between 3.5 to 28.3 nm. The temperature level is imposed in the hot and cold source using a temperature rescale method, allowing the calculation of the heat flux exchanged between the sources. Figure 2 shows the temperature profile in the longest system. The duration of the simulation to reach the steady state is 1.3 ns. In steady state, the heat flux flowing between the hot and cold sources is equal to 3.3 . $^{-2}$. The temperature profile between the sources is approximatively linear which means that the phonon mean free path is much lower than the system size, as it should since the structure is amorphous.

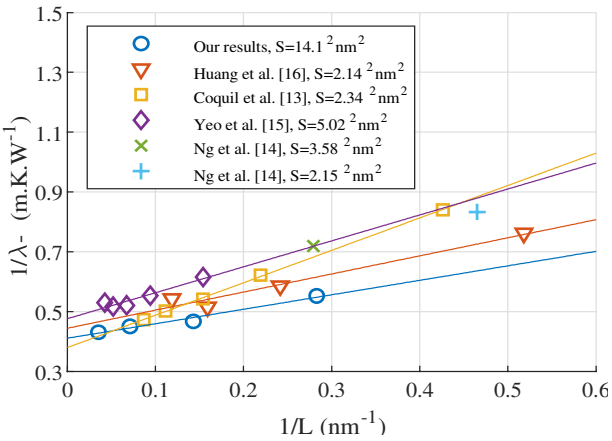

Fig.3. Inverse of the thermal conductivity function of the inverse of the system size for dense silica.

Figure 3 shows the inverse of the thermal conductivity against the inverse of the system size. The thermal conductivity increases when the system length increases. Compared to previous calculations [13–15] with the original BKS potential, our thermal conductivity values are larger. This might be due to the choice of the system section of the system which is larger than previous works. Indeed, the thermal conductivity also varies when the section of the system increases. Thus, we increased the section of our systems such that the value of the thermal conductivity does not change significantly. The thermal conductivity for an infinite length is obtained from the extrapolation of the linear fitting of the points towards $1/L = 0$; it is equal to 2.4 ± 0.1 . $^{-1}$. $^{-1}$. Despite our values for each system length being larger than previous results, the extrapolated value for the infinite system length is of the same order as the one obtained with the original BKS interatomic potential. All these values are almost twice as large as the experimental values (1.4 . $^{-1}$. $^{-1}$). Indeed, Yeo *et al.* [15] also calculated the thermal conductivity of dense silica aerogel using the Tersoff interatomic potential proposed by Munetoh *et al.* [47]. They obtained a value of the thermal conductivity equal to 1.19 . $^{-1}$. $^{-1}$. Actually, the choice of an interatomic potential to study thermal properties is not that straight. First MD simulations are classical simulations that do not account for the energy quantification of the phonon. Second, the interatomic potential should reproduce the harmonic (dispersion curves) and anharmonic behavior (phonon relaxation time) of the material. So, whatever the interatomic potential, MD simulations may result in over or under-estimation of the thermal conductivity for

temperatures lower than the Debye temperature. So, as already discussed for the choice of the interatomic potential, the optimization of computational time and the ability of the BKS interatomic potential to reproduce the surface and structural properties of silica aerogel confirm our interatomic potential choice to investigate silica aerogel thermal properties. Since the bulk thermal conductivity of silica aerogel obtained with the BKS interatomic potential is not correct, only relative variations of the thermal conductivity of silica aerogel from the bulk value will be considered.

The new methodology for the thermal conductivity prediction is used for comparison with these first results. The system is a dense amorphous silica prepared as mention in section II.B. To test the ability of the method to tackle with large systems, the volume of amorphous silica is set to $37^3 nm^3$, containing approximately 3.3 million of atoms. The initial temperature is equal to 300 K. The system is submitted to a heat flux of $1.18\, GW.m^{-2}$ during $0.78\, ns$ on the opposite sides of the sample in the x direction. With this value the temperature variation between the hot and cold sources is around 18 K, which is one order of magnitude larger than the temperature fluctuations (0.43 K).

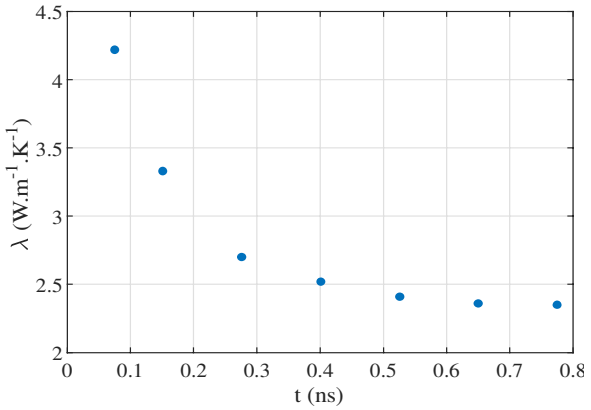

Fig.4. Identified thermal conductivity of dense silica function of the simulation duration.

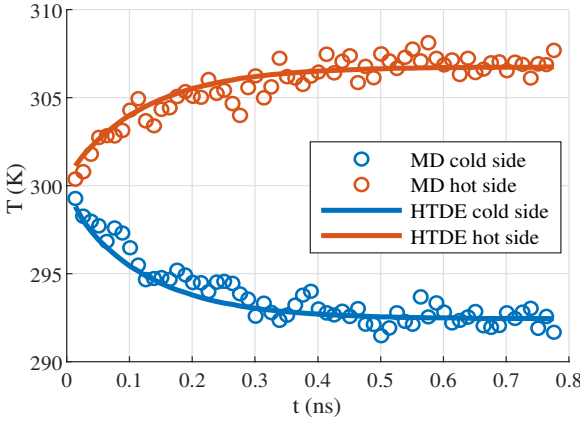

Fig.5. Temperature variation in bulk silica during heat transfer simulations, comparing MD and HTDE results for thermal conductivity identification.

Figure 4 shows the variation of the thermal conductivity against the simulation duration of the heat transfer. The thermal conductivity tends to a limit value equal to 2.35 . $^{-1}$. $^{-1}$when the simulation duration increases. This value is very close to the value obtained from the classical NEMD method. Figure 5 compares the temperature profiles obtained from the MD and HTDE simulations near the hot and cold sources. The quality of the diffusive model in dense silica is good: we find that the mean deviation D is almost equal to 1. This validates the new methodology to determine the thermal conductivity from MD simulation for amorphous material. It is thus used for silica aerogel in the remaining of the paper.

As explained in section 2.2, all big dense amorphous silica systems are constructed by replications of a small dense amorphous silica configuration which are then relaxed during $1\, ns$ at 300 K and zero stress before heat transfer simulation. After replications, the samples can be annealed at high temperature in order to eliminate possible artifacts of periodicity from replication [48]. In order to prove that our procedure of replication without annealing have no influence on the thermal conductivity, the dense amorphous silica system of dimension $14.1 \times 14.1 \times 28.3\, nm^3$ obtained by replication has been annealed at $1000\, K$ for $0.5\, ns$ then quenched to 300 K at $4.7 \times 10^{12} K.s^{-1}$ and relaxed for $0.5\, ns$. The thermal conductivity of this annealed system obtained by NEMD simulation is $2.31\, W.m^{-1}K^{-1}$ which is very close to the one previously obtained without annealing $2.32\, W.m^{-1}K^{-1}$. This confirms the reliability of our simulation strategy.

3.2. Silica aerogel

In previous studies, due to the used of the original BKS interatomic potential, the maximum system size that was considered was 20 nm, which is of the order of magnitude of the pore characteristic size in silica aerogels. Moreover, the minimum value of the density ($300 kg/\ ^3$ in Yeo *et al.* [15]) is larger than the one investigate here ($250 kg/\ ^3$). Thanks to the use of the truncated BKS interatomic potential and the new simulation strategy to determine the thermal conductivity larger systems may be considered. Our first aim is to study the influence of the system size on the thermal conductivity of silica aerogel to look for the system size that would lead to the thermal conductivity of the bulk silica aerogel. Thus, using the Kieffer's method [45], seven aerogel volumes, all with a density equal to $= 250\ .\ ^{-3}$, with different volumes are generated, $= 30^3$, 40^3, 50^3, 60^3, 70^3, 80^3 and $90^3\ \ ^3$. A heat flux of $\phi =$ 8.34, 6.57, 4.77, 4.38, 3.82, 4.08, and $4.09 \times 10^7 W.m^{-2}$ is imposed on the opposite sides of the sample. This procedure is repeated on all three directions (x, y or z) in order to induce a 1D temperature field variation.

Results are detailed for the largest system ($90^3\ \ ^3$) first. As for the dense silica, the thermal conductivity has been identified as a function of the simulation duration

(figure 6). The thermal conductivity also tends towards a limit value after $2.6ns$, a time smaller than the evaluated characteristic time τ to reach the permanent regime larger than $10ns$. However, in this case, the mean temperature deviation D is not constant and increases when the simulation duration increases (figure 6) and becomes larger than the temperature fluctuation of the MD simulation (0.53 K). The comparison between temperatures obtained from MD and HTDE simulations on figure 7 suggests that the two models (MD and HTDE) differ slightly. This disagreement might be explained by the small variation of the potential energy of the system during MD simulation due to the relaxation of the system. This effect cannot be accurately described in the HTDE but actually has a negligible influence on the value of the thermal conductivity (see discussion in appendix). Therefore, for all the systems considered hereafter, the value of the thermal conductivity is determined with the same methodology than for the dense silica.

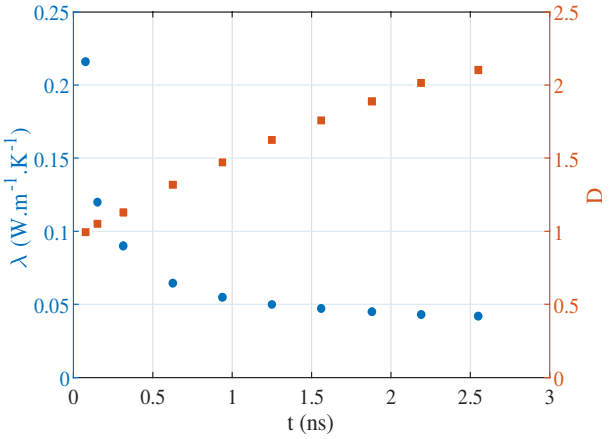

Fig.6. Thermal conductivity (point) and adimensional mean deviation D (square) versus the simulation duration.

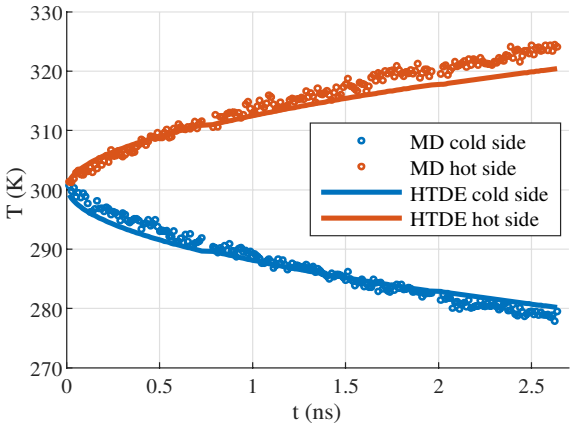

Fig.7. Temperature profile obtained from MD and HTDE for the ($90^3 nm^3$) system.

All the values of the thermal conductivities obtained for all the system sizes and directions of heat transfer are gathered on figure 8. For smaller systems, the values are quite different in the x, y and z directions while for large systems, this difference decreases and almost vanishes. As the characteristic size of the pores is $10\,nm$ then the anisotropy of the thermal conductivity for the smaller systems is due to the anisotropy of the geometry of the system. This anisotropy originates from the pore coalescence during the negative pressure cycles applied for the aerogel's generation process due to the very low target density. For larger systems, the geometry becomes isotropic, so does the thermal conductivity. This result is coherent with the one already shown by Gonçalves *et al.* [5] for the elastic modulus.

These predicted values of the thermal conductivity of silica aerogel might be quite different from the real one since, as discussed in the previous section, the prediction for dense amorphous silica is an overestimation of the experimental value. Moreover, our silica aerogel systems are quite different from real systems that have already been experimentally characterized. Real systems exhibit a two-scale organization: the nanoscale that has the same geometric characteristic than our silica aerogel and a larger scale due to the forming process of the final insulators. However, in previous studies, it has been shown that the macroscopic properties actually depend on the nanoscale. This is the case for the variation of the elastic modulus and thermal conductivity which depends on the system density [49,50]. Gonçalves *et al.* [5] has also shown that the elastic modulus power law dependence has the same exponent value as modeling or experimental studies [51–53]. So, the aim is to predict the density variation of the thermal conductivity of silica aerogel, to be compared with the experimental one.

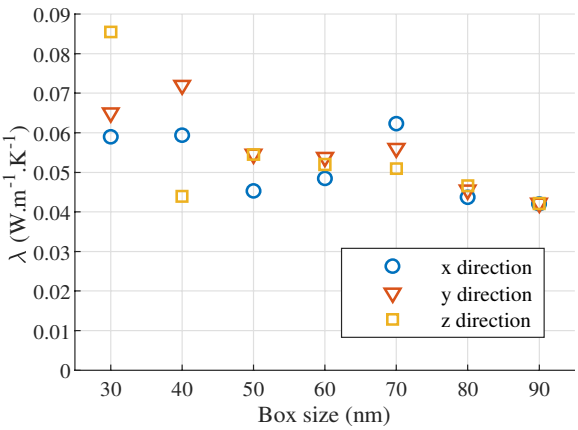

Fig.8. Thermal conductivity values obtained for different system size. The density of silica aerogel is $250kg.m^{-3}$.

Eleven aerogel systems of different densities $= 250$, 280, 320, 375, 450, 530, 660, 780, 1050, 1590 and $2255kg.m^{-3}$, with respectively volume $V = 90^3$, 74^3, 70^3, 68^3, 64^3, 60^3, 56^3, 53^3, 48^3, 42^3 and 37^3 ^{3}, are generated. The number of atoms is almost the same for all these systems. The absolute value of the heat flux imposed on each side of the simulation boxes are respectively: $\phi = 4.09, 3.81$ 3.82, 3.81, 3.90, 39.6, 40.9, 42.5, 46.2, 53.4 and $118.2 \times 10^7 W.m^{-2}$. The heat flux for systems with high density is higher in order to prevent that the temperature fluctuations are of the same order as the temperature difference imposed on each side of the simulation box. The variation of the

thermal conductivity is then plotted as a function of the system density (figure 9). For each density, the values of the thermal conductivities in the x, y and z directions are almost the same, indicating that for each density, the system size is large enough to be considered homogeneous. Also, the thermal conductivity clearly varies as a power law function of the density:

$$\lambda = a\rho^b$$

Our coefficient $b = 1.77$ is much larger than the one predicted by Ng and Yeo [14] ($b = 1.01$), for a density range from $= 320$ to $990 kg.m^{-3}$, but their system size was almost five time smaller than ours. However, note that the system size has to be large enough to ensure that the system is representative of bulk silica aerogel.

Fricke *et al.* [54] derived a model for the thermal conductivity of aerogels. Based on this model and the sound velocity measurements in aerogels Gross *et al.* [55] and Hrubesh *et al.* [56] calculated a value of b = 1.88. Thus, our value of b is in good agreement with this prediction. This coefficient b has also already been experimentally determined by Fricke *et al.* [57] and Jain *et al.* [58]. The reported experimental values of b range between 1 and 1.65. In these two papers, it has been highlighted that b strongly depends on the elaboration process.

Another empirical model has been proposed by Emmerling *et al.* [59]. It is based on the fractal dimension f_D of silica aerogels. As f_D is around 2 for the density range of interest here (around 200 . $^{-3}$) they determined a value b = 1.5, which seems to be in good agreement with experimental results [60]. However, for our silica aerogel systems, f_D varies when the density varies [5], the value of b should also varies with the density. To summarize, the relative variation of the thermal conductivity as a function of the density in our simulated silica aerogel is in good agreement with previous results. However, the comparison with experimental results is quite difficult since the interatomic potential does not allow for the real complexity of chemical interactions and chemical diversity to be reproduced.

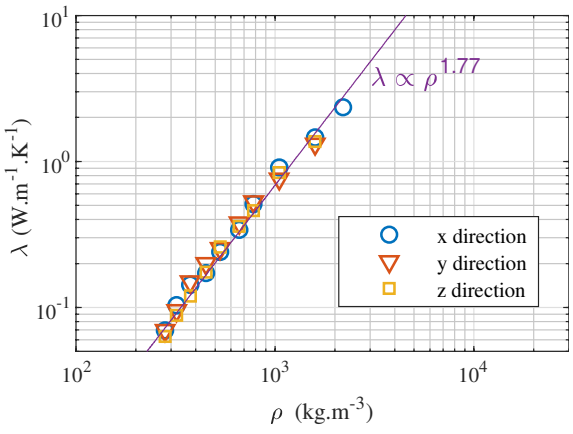

Fig.9. Thermal conductivity of silica aerogel function of the density.

4. Summary

The prediction of silica aerogel thermal conductivity is of great interest for material engineering. Due to the nanostructure of silica aerogel, the atomic description of the material is mandatory for the conduction contribution to the thermal conductivity. Molecular Dynamics simulation is an appropriate tool but the drawback of this technique is the large computational time linked to the choice of the interatomic potential and also due to the simulation strategy to predict the thermal conductivity.

In this paper, the computational time is first significantly reduced thanks to the use of the interatomic potential from Carré *et al.* [3] which has already been evaluated for MD simulation of silica aerogel mechanical properties [5,6]. Secondly, we took advantage of the diffusive nature of heat transfer in silica aerogel to propose a new methodology for the thermal conductivity prediction. It is based on the comparison of the transient temperature field given by the MD simulation and by the solution of the heat transfer diffusive equation. This new methodology makes it possible to reduce the computing time from above $10ns$ with classical NEMD to $2.6ns$ for our large systems of almost 90^3 ^{3}.

The method has been validated by comparing the prediction of the thermal conductivity of dense silica using classical NEMD and the proposed methodology. It is then used to predict the thermal conductivity of silica aerogels. The thermal conductivity of silica aerogels has been determined as a function of the system size for a density of 250 . $^{-3}$. For such a density, the average pore size is 10 nm. The anisotropy of the thermal conductivity due to the presence of pores in the aerogel decreases when the system size increases and the system may be considered isotropic when it reaches 90 nm. This is the first time such a system size has been considered for heat transfer simulation.

The thermal conductivity of silica aerogel has also been calculated as a function of the aerogel density. As expected, the thermal conductivity exhibits a power law dependence with the density. The power factor is in good agreement with the experimental results.

This new methodology to predict the thermal conductivity might be used to study materials in which conduction heat transfer is diffusive but which require the atomic description of large volume.

Acknowledgements

This work was performed using HPC resources from the FLMSN, “Fédération Lyonnaise de Modélisation et Sciences Numériques”, partner of EQUIPEX EQUIP@MESO. Funding for this project was provided by a grant from la Région Rhône-Alpes Auvergne (AURA).

References

[1] B.W.H. van Beest, G.J. Kramer, R.A. van Santen, Force fields for silicas and aluminophosphates based on *ab initio* calculations, Phys. Rev. Lett. 64 (1990) 1955–1958. doi:10.1103/PhysRevLett.64.1955.

[2] C. Rajappa, S.B. Sringeri, Y. Subramanian, J. Gopalakrishnan, A molecular dynamics study of ambient and high pressure phases of silica: Structure and enthalpy variation with molar volume, J. Chem. Phys. 140 (2014) 244512. doi:10.1063/1.4885141.

[3] A. Carré, L. Berthier, J. Horbach, S. Ispas, W. Kob, Amorphous silica modeled with truncated and screened Coulomb interactions: A molecular dynamics simulation study, J. Chem. Phys. 127 (2007) 114512. doi:10.1063/1.2777136.

[4] W. Gonçalves, J. Morthomas, P. Chantrenne, M. Perez, G. Foray, C.L. Martin, Molecular dynamics simulations of amorphous silica surface properties with truncated Coulomb interactions, J. Non-Cryst. Solids. 447 (2016) 1–8. doi:10.1016/j.jnoncrysol.2016.05.024.

[5] W. Gonçalves, J. Morthomas, P. Chantrenne, M. Perez, G. Foray, C.L. Martin, Elasticity and strength of silica aerogels: A molecular dynamics study on large volumes, Acta Mater. 145 (2018) 165–174. doi:10.1016/j.actamat.2017.12.005.

[6] W. Gonçalves, J. Amodeo, J. Morthomas, P. Chantrenne, M. Perez, G. Foray, C.L. Martin, Nanocompression of secondary particles of silica aerogel, Scr. Mater. 157 (2018) 157–161. doi:10.1016/j.scriptamat.2018.07.039.

[7] J. Lei, Z. Liu, J. Yeo, T.Y. Ng, Determination of the Young's modulus of silica aerogels – an analytical–numerical approach, Soft Matter. 9 (2013) 11367. doi:10.1039/c3sm51926k.

[8] J.S. Rivas Murillo, M.E. Bachlechner, F.A. Campo, E.J. Barbero, Structure and mechanical properties of silica aerogels and xerogels modeled by molecular dynamics simulation, J. Non-Cryst. Solids. 356 (2010) 1325–1331. doi:10.1016/j.jnoncrysol.2010.03.019.

[9] J. Yeo, Z. Liu, T.Y. Ng, Silica Aerogels: A Review of Molecular Dynamics Modelling and Characterization of the Structural, Thermal, and Mechanical Properties, in: W. Andreoni, S. Yip (Eds.), Handb. Mater. Model. Appl. Curr. Emerg. Mater., Springer International Publishing, Cham, 2018: pp. 1–21. doi:10.1007/978-3-319-50257-1_83-1.

[10] R. Coquard, D. Baillis, V. Grigorova, F. Enguehard, D. Quenard, P. Levitz, Modelling of the conductive heat transfer through nano-structured porous silica materials, J. Non-Cryst. Solids. 363 (2013) 103–115. doi:10.1016/j.jnoncrysol.2012.11.053.

[11] G. Wei, Y. Liu, X. Zhang, F. Yu, X. Du, Thermal conductivities study on silica aerogel and its composite insulation materials, Int. J. Heat Mass Transf. 54 (2011) 2355–2366. doi:10.1016/j.ijheatmasstransfer.2011.02.026.

[12] L. Roiban, G. Foray, Q. Rong, A. Perret, D. Ihiawakrim, K. Masenelli-Varlot, E. Maire, B. Yrieix, Advanced three dimensional characterization of silica-based ultraporous materials, RSC Adv. 6 (2016) 10625–10632. doi:10.1039/C5RA26014K.

[13] T. Coquil, J. Fang, L. Pilon, Molecular dynamics study of the thermal conductivity of amorphous nanoporous silica, Int. J. Heat Mass Transf. 54 (2011) 4540–4548. doi:10.1016/j.ijheatmasstransfer.2011.06.024.

[14] T.Y. Ng, J.J. Yeo, Z.S. Liu, A molecular dynamics study of the thermal conductivity of nanoporous silica aerogel, obtained through negative pressure rupturing, J. Non-Cryst. Solids. 358 (2012) 1350–1355. doi:10.1016/j.jnoncrysol.2012.03.007.

[15] J.J. Yeo, Z.S. Liu, T.Y. Ng, Enhanced thermal characterization of silica aerogels through molecular dynamics simulation, Model. Simul. Mater. Sci. Eng. 21 (2013) 075004. doi:10.1088/0965-0393/21/7/075004.

[16] Z. Huang, Z. Tang, J. Yu, S. Bai, Thermal conductivity of amorphous and crystalline thin films by molecular dynamics simulation, Phys. B Condens. Matter. 404 (2009) 1790–1793. doi:10.1016/j.physb.2009.02.022.

[17] Y.-Y. Wang, Y.-B. Gao, Y.-H. Sun, S.-Y. Chen, Effect of preparation parameters on the texture of SiO2 aerogels, Catal. Today. 30 (1996) 171–175. doi:10.1016/0920-5861(96)00010-7.

[18] M.A. Aegerter, N. Leventis, M.A. Koebel, eds., Aerogels handbook, Springer, New York, 2011.

[19] S. Volz, Microscale and Nanoscale Heat Transfer, Springer-Verlag, Sebastian Volz, Berlin Heidelberg, 2007.

[20] M.P. Allen, D.J. Tildesley, Computer Simulation of Liquids, Oxford University Press, 1997.

[21] D. Frenkel, B. Smit, Chapter 4 - Molecular Dynamics Simulations, in: D. Frenkel, B. Smit (Eds.), Underst. Mol. Simul. Second Ed., Second Edition, Academic Press, San Diego, 2002: pp. 63–107. doi:10.1016/B978-012267351-1/50006-7.

[22] A.J.C. Ladd, B. Moran, W.G. Hoover, Lattice thermal conductivity: A comparison of molecular dynamics and anharmonic lattice dynamics, Phys. Rev. B. 34 (1986) 5058–5064. doi:10.1103/PhysRevB.34.5058.

[23] R. Zwanzig, Time-Correlation Functions and Transport Coefficients in Statistical Mechanics, Annu. Rev. Phys. Chem. 16 (1965) 67–102. doi:10.1146/annurev.pc.16.100165.000435.

[24] J.R. Lukes, D.Y. Li, X.-G. Liang, C.-L. Tien, Molecular Dynamics Study of Solid Thin-Film Thermal Conductivity, J. Heat Transf. 122 (2000) 536. doi:10.1115/1.1288405.

[25] T. Ikeshoji, B. Hafskjold, Non-equilibrium molecular dynamics calculation of heat conduction in liquid and through liquid-gas interface, Mol. Phys. 81 (1994) 251–261. doi:10.1080/00268979400100171.

[26] P. Jund, R. Jullien, Molecular-dynamics calculation of the thermal conductivity of vitreous silica, Phys. Rev. B. 59 (1999) 13707.

[27] S. Maruyama, A molecular dynamics simulation of heat conduction in finite length SWNTs, Phys. B Condens. Matter. 323 (2002) 193–195. doi:10.1016/S0921-4526(02)00898-0.
[28] B.C. Daly, H.J. Maris, Calculation of the thermal conductivity of superlattices by molecular dynamics simulation, Phys. B Condens. Matter. 316–317 (2002) 247–249. doi:10.1016/S0921-4526(02)00476-3.
[29] C. Oligschleger, J.C. Schön, Simulation of thermal conductivity and heat transport in solids, Phys. Rev. B. 59 (1999) 4125–4133. doi:10.1103/PhysRevB.59.4125.
[30] C. Abs da Cruz, P. Chantrenne, R. Gomes de Aguiar Veiga, M. Perez, X. Kleber, Modified embedded-atom method interatomic potential and interfacial thermal conductance of Si-Cu systems: A molecular dynamics study, J. Appl. Phys. 113 (2013) 023710. doi:10.1063/1.4773455.
[31] P.K. Schelling, S.R. Phillpot, P. Keblinski, Comparison of atomic-level simulation methods for computing thermal conductivity, Phys. Rev. B. 65 (2002). doi:10.1103/PhysRevB.65.144306.
[32] R.H.H. Poetzsch, H. Böttger, Interplay of disorder and anharmonicity in heat conduction: Molecular-dynamics study, Phys. Rev. B. 50 (1994) 15757–15763. doi:10.1103/PhysRevB.50.15757.
[33] E.S. Landry, M.I. Hussein, A.J.H. McGaughey, Complex superlattice unit cell designs for reduced thermal conductivity, Phys. Rev. B. 77 (2008). doi:10.1103/PhysRevB.77.184302.
[34] S.S. Mahajan, G. Subbarayan, B.G. Sammakia, Estimating thermal conductivity of amorphous silica nanoparticles and nanowires using molecular dynamics simulations, Phys. Rev. E. 76 (2007). doi:10.1103/PhysRevE.76.056701.
[35] K. Termentzidis, S. Merabia, P. Chantrenne, P. Keblinski, Cross-plane thermal conductivity of superlattices with rough interfaces using equilibrium and non-equilibrium molecular dynamics, Int. J. Heat Mass Transf. 54 (2011) 2014–2020. doi:10.1016/j.ijheatmasstransfer.2011.01.001.
[36] N.S. Shcheblanov, B. Mantisi, P. Umari, A. Tanguy, Detailed analysis of plastic shear in the Raman spectra of SiO 2 glass, J. Non-Cryst. Solids. 428 (2015) 6–19. doi:10.1016/j.jnoncrysol.2015.07.035.
[37] D. Wolf, P. Keblinski, S.R. Phillpot, J. Eggebrecht, Exact method for the simulation of Coulombic systems by spherically truncated, pairwise r−1 summation, J. Chem. Phys. 110 (1999) 8254–8282. doi:10.1063/1.478738.
[38] C.J. Fennell, J.D. Gezelter, Is the Ewald summation still necessary? Pairwise alternatives to the accepted standard for long-range electrostatics, J. Chem. Phys. 124 (2006) 234104. doi:10.1063/1.2206581.
[39] M. Rarivomanantsoa, P. Jund, R. Jullien, Classical molecular dynamics simulations of amorphous silica surfaces, J. Phys. Condens. Matter. 13 (2001) 6707–6718. doi:10.1088/0953-8984/13/31/310.
[40] A. Roder, W. Kob, K. Binder, Structure and dynamics of amorphous silica surfaces, J. Chem. Phys. 114 (2001) 7602–7614. doi:10.1063/1.1360257.
[41] S.J. Plimpton, Fast Parallel Algorithms for Short-Range Molecular Dynamics, J. Comput. Phys. 117 (1995) 1–19.
[42] C. Zhong, H. Zhang, Q.P. Cao, X.D. Wang, D.X. Zhang, U. Ramamurty, J.Z. Jiang, Deformation behavior of metallic glasses with shear band like atomic structure: a molecular dynamics study, Sci. Rep. 6 (2016). doi:10.1038/srep30935.
[43] C. Zhong, H. Zhang, Q.P. Cao, X.D. Wang, D.X. Zhang, U. Ramamurty, J.Z. Jiang, On the critical thickness for non-localized to localized plastic flow transition in metallic glasses: A molecular dynamics study, Scr. Mater. 114 (2016) 93–97. doi:10.1016/j.scriptamat.2015.12.012.
[44] H.F. Zhou, C. Zhong, Q.P. Cao, S.X. Qu, X.D. Wang, W. Yang, J.Z. Jiang, Non-localized deformation in metallic alloys with amorphous structure, Acta Mater. 68 (2014) 32–41. doi:10.1016/j.actamat.2014.01.003.
[45] J. Kieffer, C.A. Angell, Generation of fractal structures by negative pressure rupturing of SiO 2 glass, J. Non-Cryst. Solids. 106 (1988) 336–342. doi:10.1016/0022-3093(88)90286-4.
[46] B. Chal, B. Yrieix, L. Roiban, K. Masenelli-Varlot, J.-M. Chenal, G. Foray, Nanostructured silica used in super-insulation materials (SIM), hygrothermal ageing followed by sorption characterizations, Energy Build. 183 (2019) 626–638. doi:10.1016/j.enbuild.2018.11.044.
[47] S. Munetoh, T. Motooka, K. Moriguchi, A. Shintani, Interatomic potential for Si–O systems using Tersoff parameterization, Comput. Mater. Sci. 39 (2007) 334–339. doi:10.1016/j.commatsci.2006.06.010.
[48] A.J. Cao, Y.Q. Cheng, E. Ma, Structural processes that initiate shear localization in metallic glass, Acta Mater. 57 (2009) 5146–5155. doi:10.1016/j.actamat.2009.07.016.
[49] A. Neugebauer, K. Chen, A. Tang, A. Allgeier, L.R. Glicksman, L.J. Gibson, Thermal conductivity and characterization of compacted, granular silica aerogel, Energy Build. 79 (2014) 47–57. doi:10.1016/j.enbuild.2014.04.025.
[50] K. Nocentini, P. Achard, P. Biwole, M. Stipetic, Hygro-thermal properties of silica aerogel blankets dried using microwave heating for building thermal insulation, Energy Build. 158 (2018) 14–22. doi:10.1016/j.enbuild.2017.10.024.
[51] T. Woignier, J. Primera, A. Alaoui, P. Etienne, F. Despestis, S. Calas-Etienne, Mechanical Properties and Brittle Behavior of Silica Aerogels, Gels. 1 (2015) 256–275. doi:10.3390/gels1020256.
[52] D. Wang, R. Pfeffer, Mixing and packing of binary hydrophobic silica aerogels, Powder Technol. 235 (2013) 975–982. doi:10.1016/j.powtec.2012.11.020.
[53] H.-S. Ma, A.P. Roberts, J.-H. Prévost, R. Jullien, G.W. Scherer, Mechanical structure–property

relationship of aerogels, J. Non-Cryst. Solids. 277 (2000) 127–141. doi:10.1016/S0022-3093(00)00288-X.
[54] J. fricke, E. Hummer, H.-J. Morper, P. Scheuerpflug, Proc. 2nd Int. Symp. Aerogels 24, C4, Les Editions de Physique, Les Ulis Cedex, Vacher, R., Phalippou, J., Pelous, J., and Woignier, T., 1989.
[55] J. Gross, J. Fricke, Ultrasonic velocity measurements in silica, carbon and organic aerogels, J. Non-Cryst. Solids. 145 (1992) 217–222. doi:10.1016/S0022-3093(05)80459-4.
[56] L.W. Hrubesh, R.W. Pekala, Thermal properties of organic and inorganic aerogels, J. Mater. Res. 9 (1994) 731–738.
[57] J. Fricke, X. Lu, P. Wang, D. Büttner, U. Heinemann, Optimization of monolithic silica aerogel insulants, Int. J. Heat Mass Transf. 35 (1992) 2305–2309. doi:10.1016/0017-9310(92)90073-2.
[58] A. Jain, S. Rogojevic, S. Ponoth, W.N. Gill, J.L. Plawsky, E. Simonyi, S.-T. Chen, P.S. Ho, Processing dependent thermal conductivity of nanoporous silica xerogel films, J. Appl. Phys. 91 (2002) 3275–3281. doi:10.1063/1.1448407.
[59] A. Emmerling, J. Fricke, Scaling properties and structure of aerogels, J. Sol-Gel Sci. Technol. 8 (1997) 781–788. doi:10.1007/BF02436938.
[60] P. Scheuerpflug, M. Hauck, J. Fricke, Thermal properties of silica aerogels between 1.4 and 330 K, J. Non-Cryst. Solids. 145 (1992) 196–201. doi:10.1016/S0022-3093(05)80455-7.

Appendix

Model difference between HTDE and MD simulations

For dense silica, the temperature fields calculated solving the HTDE (equations 1 and 2) and Molecular Dynamics simulations match quite well (see figure 5). Thus, the identification of the thermal conductivity is reliable. For silica aerogel, there is a difference between the HTDE solution and the MD simulation: this is shown on figure 7 and moreover the mean deviation D is larger than 1 (figure 6). Thus, one has to discuss the reason of this difference. To illustrate the discussion, the largest system (90^3 ^{3}) with the lowest density (250 . $^{-3}$) is considered. First, it is important to understand the origin of the difference between the temperature fields, since it might help to modify the model used to simulate heat transfer in the aerogel considered as a continuous medium.

The main point is that the mean temperature of the system (so its kinetic energy) during the MD varies between 300.8K and 302.1K (figure A1). This is not expected since during heat transfer simulation the same quantity of energy is given to the hot source and taken from the cold source of the system (Fig. 1a); the mean temperature of the system must remain constant during all the simulation. We also noted that during the MD simulation, the total energy is constant, which is coherent with the boundary condition for heat transfer simulation while the potential energy decreases (Figure A2) and the kinetic energy (so its temperature) increases. Thus, we think that the scenario that leads to the temperature increase is the following (Figure A3): during the simulation, the system experiences relaxations, giving rise to a decrease of potential energy by the value E_r corresponding to a virtual state of the system which correspond to the relaxed system. As the total energy of the system is constant and due to the equipartition theorem, the energy E_r due to the relaxation is given back to the system in the virtual state, half of it is transformed into kinetic energy (which is equivalent to a temperature rise) and the other part into potential energy. So, between the initial state and the final state of the simulation, the kinetic energy increases while the potential energy decreases. For the heat transfer model, this is equivalent to add a term source in the HTDE:

$$\rho c \frac{\partial T_s(x,t)}{\partial t} = \lambda \frac{\partial^2 T_s(x,t)}{\partial x^2} + g$$

Using the time variation of the temperature and potential energy, it is possible to identified a source term function of time. To identify the thermal conductivity, the only change to do in the methodology is to add the source term in the HTDE.

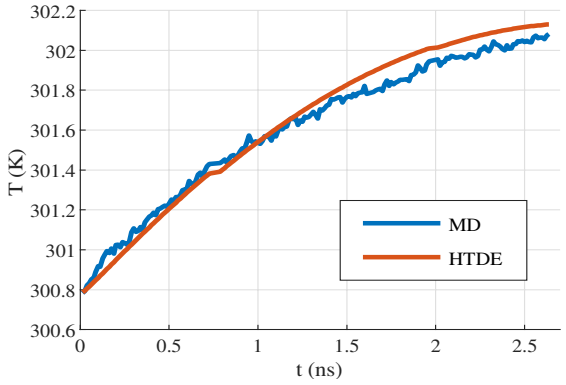

Fig.A1. Mean temperature of the system obtained from the solution of the HTDE with the source term compared to MD mean temperature.

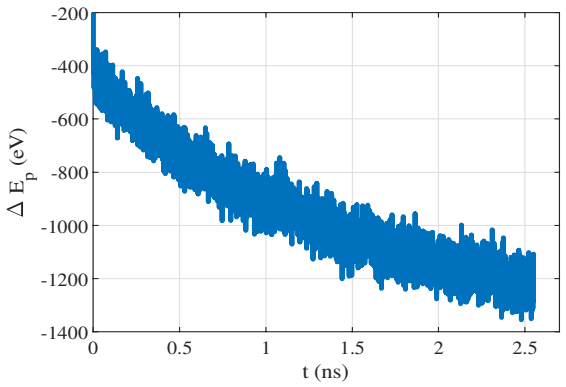

Fig.A2. Potential energy variation of the system during MD heat transfer simulation.

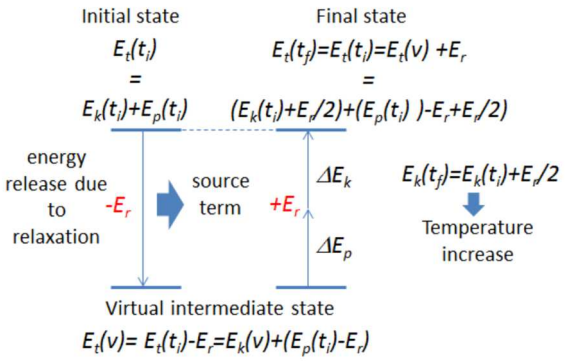

Fig.A3. Principle of the energy variation during the transient NEMD simulation.

The results are shown on figure A4 and compared to the one obtained without the source term. Accounting for the source term do not change the value of the thermal conductivity, but it decreases significantly the mean deviation D. However, D is still larger than 1. To our point of view, this is due to the fact that in our model, the source term is homogeneous while in MD simulation, this source term is due to local relaxation. This is however not possible to describe the spatial variation of the source term. So, there will always be a model difference between the HTDE and the MD simulation. The figure A5 confirms this assumption: the new temperature histories near the heat sources with MD simulation and the solution of HTDE with the source term exhibit a better agreement near the hot source and it seems that the agreement is less good near the cold source (see figure 7 for the same comparison without the source term) : due to the local nature of the source term it is not possible to have a perfect agreement between the two solutions in the whole system.

Fig.A4. Thermal conductivity and mean deviation D as a function of the simulation duration without (points and filled squares) or with (circles and empty squares) source term.

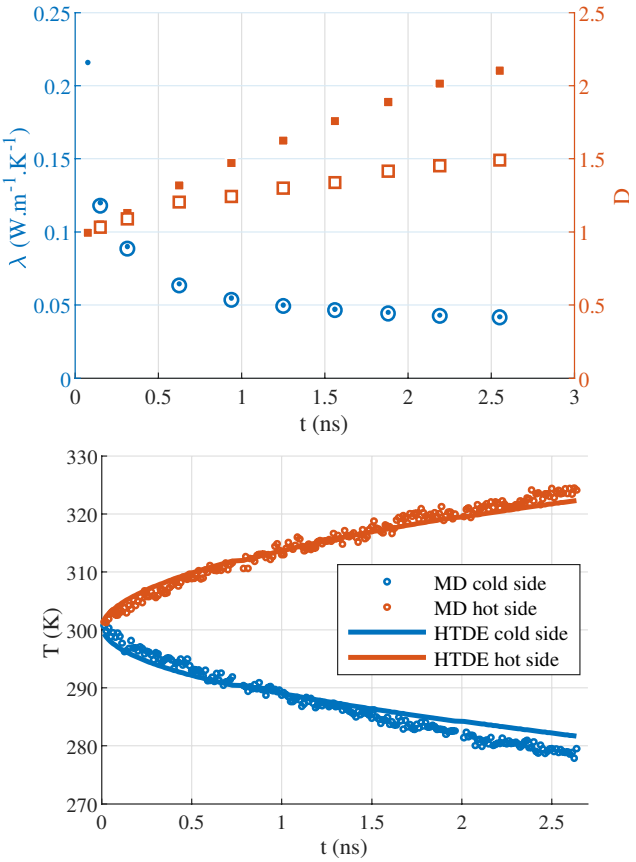

Fig.A5. Temperature history near the hot and cold sources. Comparison between MD results and the HTDE with source term.

As a conclusion, it is clear that the value of the thermal conductivity does not change if the term source is considered or not in the HTDE (several tests have been done for other system sizes and density), thus the results for the thermal conductivity are all obtained solving equation 1 of the paper without the source term.